

Protein-responsive gut hormone Tachykinin directs food choice and impacts lifespan in *Drosophila*

Kim Rewitz (✉ Kim.Rewitz@bio.ku.dk)

University of Copenhagen <https://orcid.org/0000-0002-4409-9941>

Nadja Ahrentlov

University of Copenhagen

Olga Kubrak

University of Copenhagen

Alina Malita

University of Copenhagen

Takashi Koyama

University of Copenhagen <https://orcid.org/0000-0003-4203-114X>

Alphy John

University of Copenhagen <https://orcid.org/0000-0003-1319-3799>

Pernille Madsen

University of Copenhagen

Kenneth Halberg

University of Copenhagen <https://orcid.org/0000-0002-5903-7196>

Stanislav Nagy

University of Copenhagen

Michael Texada

University of Copenhagen <https://orcid.org/0000-0003-2479-1241>

Article

Keywords:

Posted Date: January 16th, 2024

DOI: <https://doi.org/10.21203/rs.3.rs-3837414/v1>

License: © ⓘ This work is licensed under a Creative Commons Attribution 4.0 International License.

[Read Full License](#)

Additional Declarations: There is **NO** Competing Interest.

Protein-responsive gut hormone Tachykinin directs food choice and impacts lifespan in *Drosophila*

Nadja Ahrentlöv¹, Olga Kubrak¹, Alina Malita¹, Takashi Koyama¹, Alphy John¹, Pernille E. H. Madsen¹, Kenneth V. Halberg¹, Stanislav Nagy¹, Michael J. Texada¹, Kim Rewitz^{1,*}

¹ Department of Biology, University of Copenhagen, 2100 Copenhagen O, Denmark

*Correspondence: Kim.Rewitz@bio.ku.dk

Abstract

Animals select food based on hungers that reflect dynamic and specific macronutrient needs. Feeding behavior is governed by endocrine signals, but the hormonal mechanisms underlying nutrient-specific appetite regulation are poorly defined. We demonstrate that the gut hormone Tachykinin (Tk), an ortholog of mammalian Substance P, controls selective appetite regulation in *Drosophila*. When protein-rich food is consumed, enteroendocrine cells (EECs) of the midgut release Tk, which acts on adipokinetic hormone (AKH)-producing cells. AKH suppresses protein appetite and enhances sugar hunger, thus forming an endocrine feedback system that aligns food choice with the internal nutritional state. Inhibiting this protein-responsive gut hormone increases fecundity and also prolongs lifespan through AKH, revealing a role of nutrient-dependent gut-hormone signaling in influencing longevity. Our results provide the framework for understanding EEC-derived nutrient-specific satiety signals and the role of gut hormones in the regulation of food choice and lifespan.

Introduction

Animals' survival depends on their ability to adapt their feeding behavior to changing internal nutritional conditions. This homeostatic regulation of food intake is governed by neural and endocrine signals that control appetite or feeding drive, ensuring a balance between total energy intake and expenditure¹. Furthermore, it has become clear that such mechanisms govern not only animals' general appetite but also their preferences for foods containing specific macronutrients, as a way to satisfy physiological needs² and to maintain proper balance between individual nutrients. Central to this balancing is the ability of animals to select food with the specific nutrients they require. Food selection is driven by "specific appetites" for distinct nutrients, a phenomenon exhibited across animal species, including in humans¹⁻³. Nonspecific appetite is understood to be governed by hormonal signaling, with many endocrine factors known to contribute to general hunger and satiety regulation. However, the endocrine signals that control nutrient-specific appetite and food choice, which are key aspects of homeostatic feeding behavior, remain unclear. An essential component of these regulatory mechanisms is that the intake of a given macronutrient must be sensed in some way to drive nutrient-specific negative feedback that decreases future preference for the ingested nutrient. In line with this, we recently found that the hormone Neuropeptide F (NPF) is released from endocrine cells of the mated female *Drosophila* gut in direct response to these cells' detection of consumed sugar. This hormone targets neurosecretory cells, providing them with the feedback necessary to suppress sugar appetite⁴. Thus, sugar-induced gut NPF induces a sugar-satiety mechanism, balancing sugar consumption.

Dietary protein intake influences growth, metabolism, fecundity, and lifespan across species. However, the mechanisms that selectively regulate the ingestion of protein remain poorly understood. The protein leverage hypothesis suggests that animals, including humans, prioritize protein intake over other macronutrients such as carbohydrates and fats when making dietary choices, and thus consume available food until protein need is satisfied. In the context of modern diets, in which low-protein but high-calorie foods are prevalent, this often leads to overconsumption of accompanying sugars and fats along the path to protein satiety^{5,6}. This behavioral response represents a form of homeostatic food selection, by which the organism adjusts its food choices based on protein requirements. When dietary protein intake is insufficient, the resulting internal state can modulate feeding behaviors to favor protein consumption to restore balance and ensure optimal physiological function. In mice, protein restriction has been shown to shift preference toward protein-containing food. This response is regulated at least in part by FGF21, a liver-derived endocrine signal that acts on the brain to adapt feeding behavior⁷. Similarly, the fruit fly *Drosophila* modulates its food choices based on its internal state². In mammals, liver FGF21 is upregulated under low-protein feeding via the transcription factor ATF4, and a similar ATF4-dependent adaptive endocrine response has been identified in the fly equivalent of the mammalian liver and adipose tissue to counter protein restriction⁸.

In *Drosophila*, signals from peripheral organs play a large role in controlling appetite, with specialized endocrine cells of the gut (enteroendocrine cells, EECs) gaining attention for their functions in governing feeding behavior and metabolism^{3,4,9-12}, paralleling extensive human research. These endocrine cells produce diverse hormones that signal to the brain to adjust feeding behavior based on the nutritional status of the gut. Indeed, therapies centered around the human EEC-derived glucagon-like peptide 1 (GLP-1) have shown great potential in appetite reduction for weight loss¹³. In *Drosophila*, the gut-brain axis was recently found to detect deficiencies in essential amino acids and to induce a compensatory appetite for these nutrients¹⁰. However, in this case it is the absorptive enterocytes, rather than the EECs, that sense the lack of diet- and microbiome-derived amino acids, releasing the peptide CNMamide (CNMa), which signals the brain to induce amino-acid-specific hunger. Although both FGF21 and CNMa induce a preference for protein-rich food under protein-deficiency conditions, the mechanisms activated by protein intake that induce protein-specific satiety remain unidentified.

Here we present our findings showing that certain EECs of the adult female *Drosophila* midgut produce the conserved gut hormone Tachykinin (Tk), an ortholog of mammalian Substance P. Upon sensing protein-rich food intake, these cells release Tk, which acts on cells producing the glucagon-like factor adipokinetic hormone (AKH) to suppress further intake of protein-rich food while promoting sugar consumption, forming a feedback loop that drives homeostatic nutrient consumption. Furthermore, inhibiting this protein-responsive Tk in the gut extends lifespan in an AKH-dependent

manner. These discoveries advance our understanding of how gut-mediated protein sensing regulates food choices for nutritional balance and how the gut influences lifespan.

Results

Gut-derived hormone *Tk* modulates dietary choices in response to macronutrient intake

We recently found, together with our colleagues, that sugar consumption triggers the release of gut NPF, which in turn curbs the appetite for sugar and adjusts systemic sugar metabolism^{4,12}. Interested in whether animals also modulate their protein intake based on their internal state, we decided to examine their dietary choices in that respect. We allowed mated female flies to consume either a protein-rich diet (10% yeast) or a sugar diet (10% sucrose) for 15 hours to induce sugar or protein satiety, respectively. We then measured the amount of 10% yeast or 10% sucrose each animal consumed during a one-hour short-term dye-consumption assay. Sugar-fed animals exhibited a decreased intake of the sugar diet compared to those that had consumed a yeast diet, which displayed an increased appetite for sugar (Fig. 1a). These observations are consistent with our findings that dietary sugar is sensed by the NPF⁺ EECs, leading to the suppression of appetite for this nutrient⁴. Intriguingly, a similar effect was observed for protein consumption: yeast-fed animals consumed less when subsequently presented with protein-rich food compared to those that had previously consumed sugar (Fig. 1a). This suggests that animals adjust their consumption of protein and sugar based on their recent intake of both of these nutrients, aiming for a balanced diet.

Our findings led us to ask whether this protein-satiety effect was triggered by gut-mediated amino-acid detection. We focused on *Tk*, a hormone reported to be expressed in a subset of EECs in the adult midgut that are responsive to amino acids¹⁴, to investigate whether this factor plays a role in the increased sugar appetite and reduced protein appetite observed after protein consumption. To uncover the mechanism directing feeding responses upon detection of consumed protein, we fed mated females a 10% yeast diet for 15 hours prior to feeding tests to induce protein satiety and hunger for dietary sugar in all subsequent experiments, unless specified otherwise. Animals with *Tk* knockdown in the *Tk*-expressing EECs consumed less sugar (Fig. 1b), while they ingested high amounts of protein food despite their recent *ad-libitum* intake of yeast food (Fig. 1c). We observed similar effects with two independent RNAi lines, ruling out off-target effects. We further demonstrated that our approach specifically targets *Tk* in the gut, without affecting *Tk* expression in the nervous system, where it is also produced. This specificity towards gut-derived *Tk*, as opposed to neuronal *Tk*, was demonstrated by the lack of detectable brain expression of *UAS-GFP* induced by our driver line (*Tk::2A::GAL4* combined with pan-neuronal *R57C10-GAL80* to inhibit neuronal GAL4 activity³, a combination hereafter referred to as *Tk^{gut}>*) (Fig. 1d). Using this setup to drive RNAi against *Tk* strongly reduced *Tk* expression in the midgut without inducing detectable neuronal knockdown (Fig. 1e). We also excluded the possibility that the UAS transgene itself might have influenced the sugar-feeding phenotype, by crossing the *UAS-Tk-RNAi* (*Tk-RNAi*) line with the *w¹¹¹⁸* control background. The results from this UAS-only genotype were consistent with those from the *Tk^{gut}>* driver-only control (Extended Data Fig. 1a).

We next confirmed the decreased-sugar-appetite phenotype using a longer-term food consumption assay (capillary feeder, CAFÉ¹⁵) and an automated behavior-monitoring system (FLIC) that tracks how often and for how long single animals interact with sugar-only liquid food¹⁶. As they did in the short-term food consumption assay, yeast-satiated females expressing gut-specific *Tk* knockdown consumed less sugar over a 6-hour period and exhibited reduced feeding time on sugar food compared to control animals (Fig. 1f,g), including UAS-only genotypes (Extended Data Fig. 1b,c). To further confirm the regulation of sugar and protein feeding by gut *Tk*, we used another automated system, the FlyPAD apparatus, that allows the detection of individual sips of sugar- or protein (yeast)-containing solid food as well as the measuring of animals' preference between these nutrients¹⁷. In line with our previous observations, yeast-fed females with gut-specific *Tk* knockdown exhibited a decrease in sugar feeding accompanied by elevated protein feeding (Fig. 1h,i) and displayed an increase in preference for the protein-rich food when presented with both media in a two-choice assay (Fig. 1j). Collectively, these findings imply that the observed feeding phenotypes arise from the EEC-specific loss of *Tk*. They further suggest that gut *Tk* serves as a satiety signal that is required after a protein-rich meal for curbing further protein intake and for promoting appetite towards carbohydrate-rich food. To assess whether gut-derived *Tk* inhibits protein consumption, we introduced the thermosensitive cation

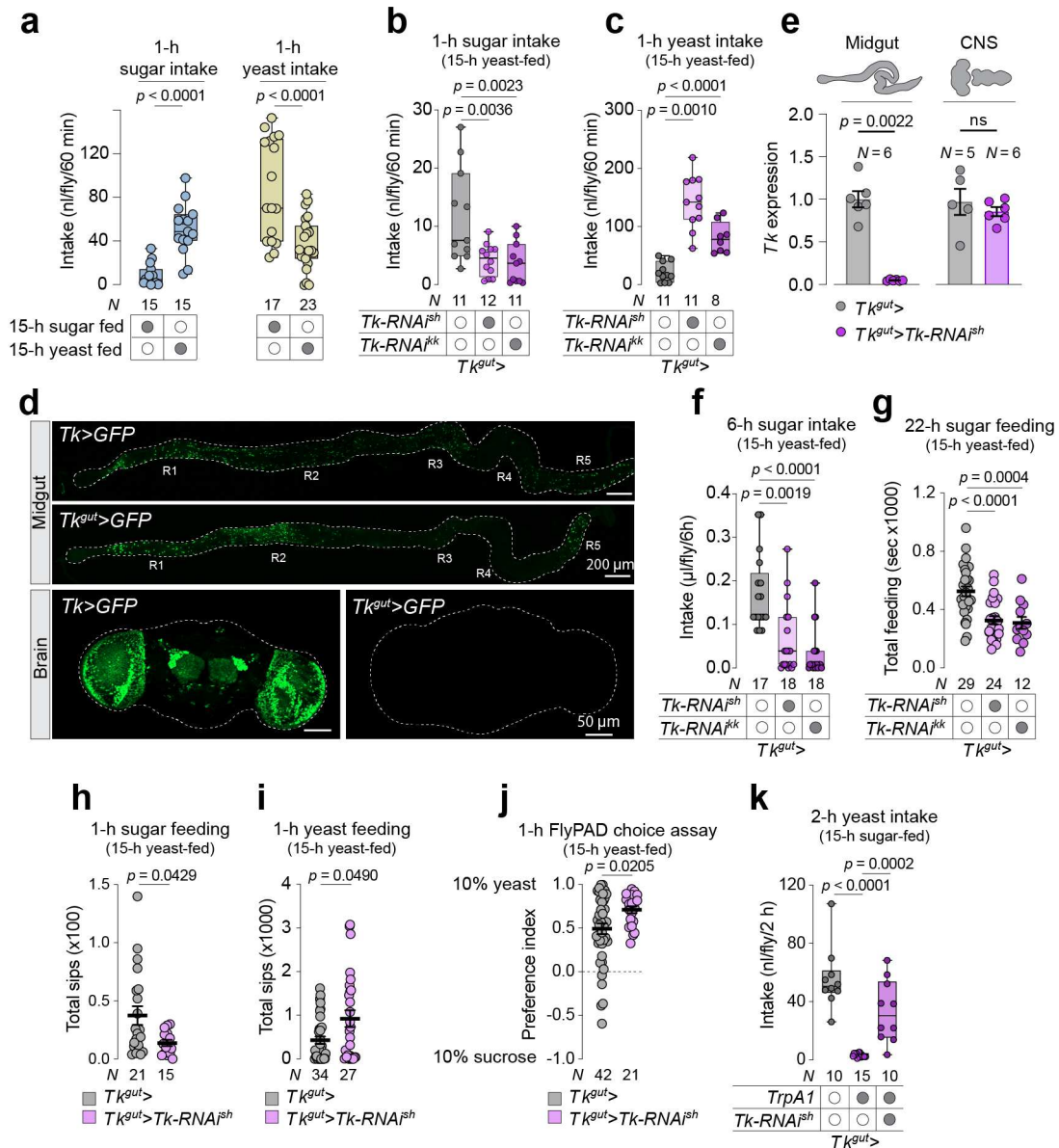


Figure 1. Gut-derived Tk affects selective appetite by increasing sugar intake and suppressing protein consumption in mated females. **a**, Intake of sugar and yeast over a one-hour test in flies that were previously fed on a sugar diet for 15 hours compared to those fed on a yeast diet for the same period. Statistical significance was assessed by two-tailed unpaired Student's t test. **b-c**, One-hour intake of sugar (**b**) and yeast (**c**) for flies previously fed for 15 h on a yeast diet. Statistical significance determined by one-way ANOVA with Dunnett's multiple comparisons test. **d**, Representative confocal images of *UAS-mCD8::GFP* (*UAS-GFP*) expression in the midgut (upper panel) and brain (lower panel) driven by *Tk::2A::GAL4* (*Tk>*) and *Tk>* in combination with *R57C10-GAL80* (*Tk^{gut>}*), which suppresses neuronal GAL4 activity. Scale bars: 200 μm (midgut), 50 μm (brain). **e**, *Tk* expression levels in the midgut and central nervous system (CNS) of control *Tk^{gut>}* and *Tk^{gut>}Tk-RNAi* flies. Expression is significantly reduced in the midgut of knockdown flies, assessed by Mann-Whitney U test. **f-g**, Long-term intake of sugar (**f**) and yeast (**g**) in flies following 15-hour yeast-diet feeding. Statistical significance assessed using Kruskal-Wallis test with Dunn's multiple comparisons test (**f**) and one-way ANOVA with Dunnett's test (**g**). **h-i**, Total sips from sugar (**h**) and yeast (**i**) media measured by FlyPAD assay over one hour for flies previously fed on a 15-hour yeast diet, with significant differences between the groups determined by Mann-Whitney U test. **j**, Preference index for yeast over sugar in the two-choice FlyPAD assay following 15-hour yeast-diet feeding. Statistical difference determined by Mann-Whitney U test. **k**, Two-hour intake of yeast in flies with *TrpA1* activation of *Tk⁺* EECs, with and without simultaneous *Tk-RNAi*. Statistical analysis by one-way ANOVA with Dunnett's test. Sample sizes (N) and *p* values are indicated in each plot. **a, b, c, f, g, k**: Box plots indicate minimum, 25th percentile, median, 75th percentile, and maximum values. **e, g, h, i, j**: Data are presented as mean \pm SEM. ns, non-significant ($p > 0.05$).

channel Transient receptor potential A1 (TrpA1)¹⁸ into Tk⁺ EECs, permitting induction of Tk release. We conditioned mated females by providing them with sugar-based food for 15 hours, thereby priming their appetite for a protein-rich diet. During the last two hours of this period, the animals were incubated at 29 °C to trigger TrpA1-induced Tk release. This manipulation resulted in the complete inhibition of protein intake, despite the animals' being fed only sugar for the preceding 15 hours (15 h protein-deprivation; Fig. 1k), a treatment that induces control animals to consume yeast (Fig. 1a). Since Tk⁺ EECs express multiple peptides, and TrpA1 activation presumably leads to the release of all of them, we tested whether the observed effect requires Tk. Concurrent *Tk* knockdown attenuated the protein-aversion phenotype of TrpA1 induction, indicating that Tk itself is indeed required. Together these results demonstrate that EEC-derived Tk can suppress protein appetite, even under a condition in which this appetite is normally strongly upregulated.

Enteroendocrine hormones are also known for their role in modulating metabolism, and metabolic status is also a strong influence on feeding behavior, raising the possibility that the observed feeding changes arise in response to Tk-induced metabolic shifts rather than as a direct response to Tk-mediated signaling. We thus asked whether gut Tk might affect nutrient storage or metabolism. Animals expressing gut-specific *Tk* knockdown displayed no alteration in whole-body triacylglyceride (TAG) levels under fed conditions (Extended Data Fig. 1d). However, there was a small decrease in lipid depletion during starvation, suggesting slower mobilization, which was consistent with these animals' slightly prolonged survival during starvation (Extended Data Fig. 1e). These findings support the idea that the observed effects of Tk on feeding arise directly through Tk-driven effects on behavioral centers, rather than their being secondary effects of metabolic perturbations.

Dietary protein activates Tk-positive enteroendocrine cells and induces Tk release

EECs can sense dietary nutrients, and the EECs of the posterior midgut of the fly are activated by dietary amino acids¹⁴. Since the EEC-specific knockdown of *Tk* led to phenotypes that are consistent with the hormone's being released in response to protein intake, we investigated whether Tk⁺ EECs are indeed activated by protein-rich food. We employed the CaLexA reporter system, in which *GFP* expression, reflective of recent calcium-signaling activity history¹⁹, enables the measurements of EEC activity in freely moving animals (Fig. 2a). Although the release of Tk from midgut EECs has been linked with starvation²⁰, we did not observe any activation of Tk⁺ EECs or change in their intracellular Tk peptide levels after a short-term (4-h) period of fasting (Extended Data Fig. 2a,b). In contrast, under prolonged starvation (11 hours), both the calcium activity of Tk⁺ EECs and their intracellular Tk peptide levels were reduced compared to those seen in fed conditions (Extended Data Fig. 2c,d). This implies that starvation conditions may enhance gut Tk release through some means other than calcium-evoked release, consistent with previous findings indicating that starvation enhances Tk production in midgut EECs.

We then asked whether short-term feeding with either sugar or yeast would influence Tk⁺ EEC activity and Tk peptide release. To observe short-term responses, we fasted animals for 25 h beforehand to stimulate feeding drive and then refed them with sugar or yeast medium for 3 hours. We found that intracellular Tk peptide levels in yeast-refed animals were lower than those seen in sugar-fed animals (Extended Data Fig. 2e,f). This effect was not linked to any changes in *Tk* transcript levels, and no transcriptional *Tk* changes were observed even after 6 h of feeding on standard food containing both sugar and yeast (Extended Data Fig. 2g,h). Thus, the low Tk peptide levels observed after 3 h of yeast refeeding are likely caused by greater release of Tk under these dietary conditions, although this again was not accompanied by any significant change in the cells' calcium activity, perhaps due to the relatively short period. We therefore examined the effects of prolonged feeding and found that both calcium activity in Tk⁺ EECs and Tk peptide levels were significantly affected. After 18 hours of feeding on protein-rich yeast, Tk peptide levels within the EECs was again low, but with the extended feeding period, the calcium activity in the Tk⁺ EECs was elevated (Fig. 2b,c). This suggests that Tk⁺ EECs are more responsive to dietary protein food than to sugar food.

We then investigated whether yeast feeding might differentially activate the Tk⁺ EECs of the anatomically and functionally distinct regions (named R1-R5) of the midgut. We observed that after extended (15-hour) yeast feeding, the Tk⁺ EECs throughout the gut exhibited increased calcium activity compared to sugar-fed conditions. This was correlated with decreased Tk peptide levels across all regions (R1-R5), with a pronounced effect observed in R5 (Fig. 2d,e). These observations imply that

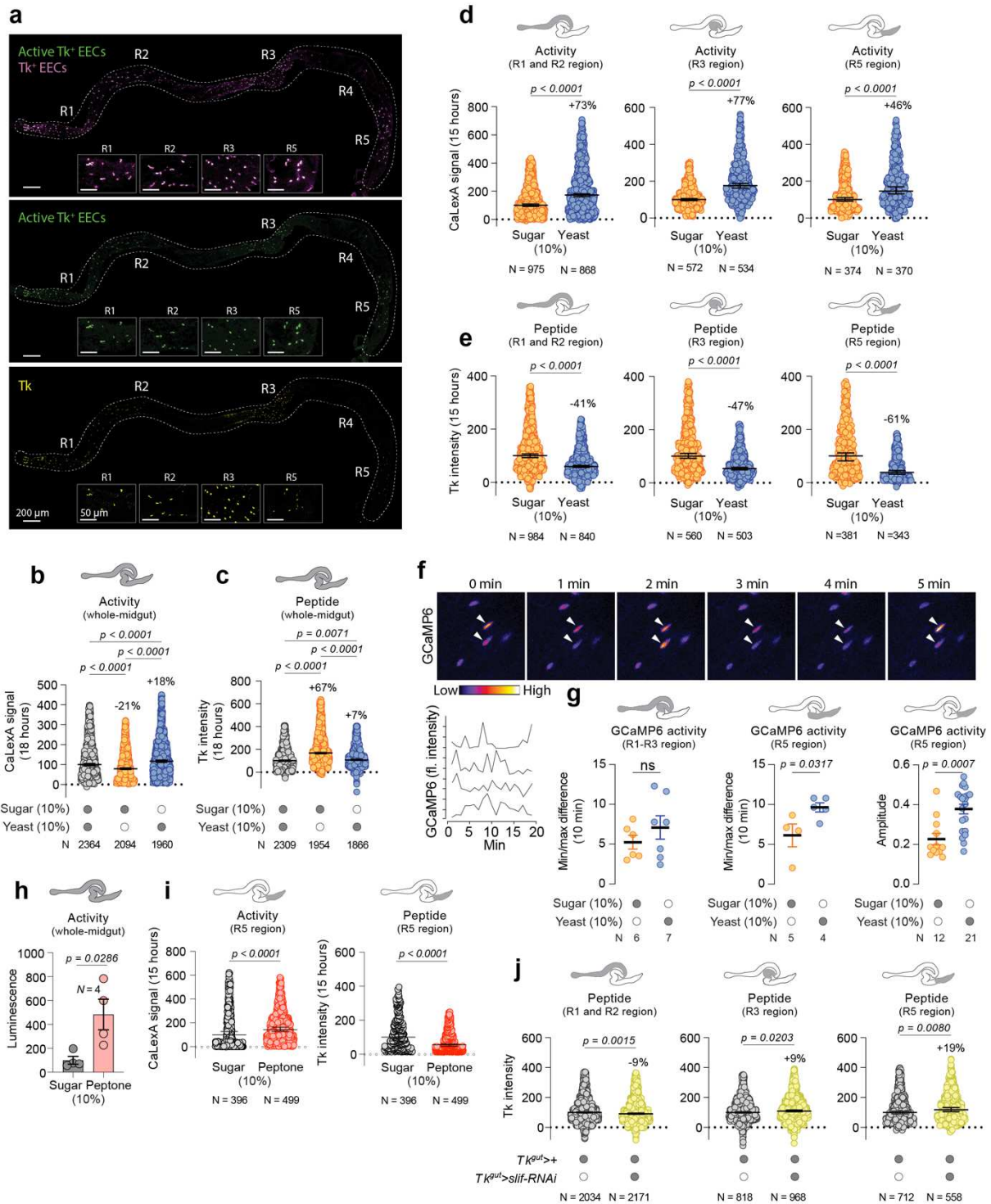


Figure 2: Macronutrient consumption modulates Tk^+ EEC activity and Tk peptide release in mated females. **a**, Representative confocal images of Tk^+ EECs of the midgut expressing the activity reporter CaLexA of flies fed adult-optimized food (containing 9% sugar and 8% yeast and 1% agarose). Top: Active Tk^+ EECs are shown in green (*CaLexA*>*GFP*), and all Tk^+ EECs are labeled with magenta (tdTomato). Middle: Active Tk^+ EECs (*CaLexA*>*GFP*). Bottom: Antibody staining of Tk peptide. Insets: gut R1-R5 segments. Scale bars, 200 μ m (whole midgut) and 50 μ m (insets). **b-c**, Quantification of calcium-dependent activity (ratio of GFP to tdTomato) in Tk^+ EECs as a proxy for activity throughout the whole midgut (**b**) and measurement of anti- Tk staining intensity (**c**) in flies fed for 15 hours with sugar, yeast, or both. Significance determined by Kruskal-Wallis test with Dunn's multiple comparisons test. **d-e**, Region-specific CaLexA analysis of Tk^+ EECs (**d**) and Tk peptide staining intensity (**e**) in midgut regions R1+R2, R3, and R5 following 15 hours' feeding on sugar or yeast diet. Significance determined by Mann-Whitney U tests. **f-g**, Dynamic GCaMP6 activity in Tk^+ EECs following ingestion of sugar

or yeast in the R1-3 and R5 regions of the midgut over a 20-minute period. (f) Representative GCaMP fluorescence-intensity plots indicating activation patterns. (g) Differences between minimum and maximum fluorescence intensity and amplitude differences in GCaMP6 activity between sugar and yeast diets in different regions of the midgut. The amplitude of calcium fluctuations was quantified through non-linear regression analysis of the GCaMP fluorescence intensity, employing a standard sine-wave model in PRISM software. Significance was determined with Mann-Whitney U tests. (h) Tk-cell calcium activity in midguts from flies fed 15 hours with sugar or Bacto peptone (4 dissected midguts per replicate) using a luciferase-based CaLexA calcium-reporter system (*Tk>LexA::NFAT::VP16; LexAop-Luciferase*). Significance was determined with Mann-Whitney U tests. (i) Calcium-dependent GFP activity (GFP/tdTomato ratio) in Tk⁺ EECs in the R5 region and anti-Tk staining intensity in flies fed for 15 hours with sugar or Bacto peptone. Significance was determined with Mann-Whitney U tests. (j) Changes in Tk peptide-staining intensity in the R1+R2, R3, and R5 regions of *Tk^{gut}>* controls and *Tk^{gut}>slif-RNAi* animals, with significance determined by Mann-Whitney U test. Sample sizes (N) and *p* values are indicated in each plot. Data are presented as mean ± SEM. ns, non-significant (*p*>0.05).

protein-rich food induces the release of Tk from Tk⁺ EECs throughout the midgut, with strong effects in the posterior region. We next established an *ex-vivo* midgut setup for calcium imaging and employed *Tk::2A::GAL4* to express *GCaMP6s*²¹, a genetically encoded calcium sensor, in Tk⁺ EECs. Our findings revealed that both the range and amplitude of GCaMP signals in the Tk⁺ EECs of the posterior-most region, R5, were enhanced when animals had been fed with yeast prior to observations, compared to sugar feeding (Fig. 2f,g). To verify that amino acids are dietary components that influence the activity of Tk⁺ cells in EECs and the levels of Tk peptide within these cells, we provided the flies with diets of either sucrose or peptone, each serving as the exclusive source of sugar and protein. Tk⁺ EECs exhibited increased calcium activity in the midgut when animals were supplied with peptone food compared to sugar food, as determined using a modified CaLexA reporter system in which expression of Luciferase rather than GFP reflects recent calcium-signaling activity^{3,22} (Fig. 2h). We next investigated whether Tk⁺ EECs in the R5 region in particular are responsive to dietary protein by using the GFP-based CaLexA reporter system. Our findings revealed that the calcium activity of region-5 Tk⁺ EECs indeed increased in animals fed with peptone compared to those fed with sugar (Fig. 2i). This increase in activity coincided with reduced levels of Tk peptide, collectively suggesting that dietary protein activates midgut Tk⁺ EECs, prompting the release of Tk.

Since these data indicate that Tk is released in response to protein feeding, we asked whether cell-autonomous amino-acid sensing in the Tk⁺ EECs affects Tk release. Based on available single-cell sequencing data²³, the amino-acid transporter Slimfast (Slif), which plays a role in amino-acid sensing in the fat body²⁴, is expressed in a subset of Tk⁺ EECs²³. Knocking down *slif* in the Tk⁺ EECs resulted in intracellular accumulation of Tk peptide, primarily in the R3 and R5 segments, with the most significant effect observed in R5, whereas no accumulation was observed in the anterior R1/R2 segments (Fig. 2h). No changes in *Tk* transcript levels were detected when whole midguts were assessed (Extended Data Fig. 2j), suggesting that the observed increase in intracellular Tk levels is a consequence of peptide retention. We also found that, when *slif* knockdown was targeted solely to the Tk⁺ gut endocrine cells, the level of *slif* transcripts in whole-gut samples decreased, indicating that *slif* is expressed in Tk⁺ EECs (Extended Data Fig. 2j). Furthermore, silencing *slif* in Tk⁺ EECs led to a small increase in resistance to starvation (Extended Data Fig. 2k), similar to the effect observed with gut *Tk* knockdown (Extended Data Fig. 1d). Collectively, our findings from both yeast-feeding experiments and *slif* knockdown in the Tk⁺ EECs suggest that the consumption of protein-rich food activates Tk⁺ EECs, leading to the release of the Tk peptide. This release mechanism appears to involve Slif-dependent amino-acid sensing, at least in the posterior portion of the midgut. Indeed, animals with knockdown of *slif* in the Tk⁺ EECs displayed reduced sugar intake over a one-hour period following 15 h of yeast-only feeding (Extended Data Fig. 2l), mirroring the behavior of animals with EEC-targeted *Tk* knockdown (Extended Data Fig. 1a). However, these animals exhibited no accompanying alteration in yeast feeding (Extended Data Fig. 2m), implying that the absence of Slif does not fully phenocopy *Tk* loss. This is consistent with the results showing that *slif* loss leads to Tk retention primarily in posterior midgut segments, whereas protein consumption induces Tk release from all regions. Alternatively, the knockdown of *slif* might affect the release of other gut hormones in addition to Tk, given that Tk⁺ EECs also produce both NPF and Diuretic hormone 31 (Dh31)^{25,26}. In any case, our

findings suggest that Slif-mediated amino-acid sensing is involved in the regulation of Tk release from EECs.

Gut Tk regulates glucagon-like signaling

To pinpoint the target tissue(s) through which gut Tk influences behavior, we examined the expression of its cognate receptor, *TkR99D*. We found that this receptor is broadly expressed in the central nervous system, with notable expression in the neuroendocrine cells that produce AKH (AKH-producing cells, APCs; Fig. 3a), a glucagon-like hormone. AKH acts on the fat body – an organ comparable to the mammalian liver and adipose tissue – to induce the breakdown and release of stored energy during periods of starvation^{3,27-30}. We recently discovered that the release of AKH from APCs is enhanced by the EEC-derived peptide Allatostatin C (AstC, orthologous with mammalian somatostatin), released when nutrients are scarce³. We and others have also recently shown that the consumption of dietary sugar triggers the release of NPF from EECs^{4,12}. This gut-derived NPF inhibits AKH release and thus blocks the AKH-induced mobilization of stores, thereby allowing the consumed sugar to be taken up by the adipose tissue and stored. Furthermore, we observed that gut-derived NPF, through its regulation of AKH, can also influence food preference, regulating the choice between sugar and protein-rich yeast food⁴. We thus explored whether gut-derived Tk might also modulate AKH release and, if so, whether this mechanism might mediate the observed Tk-driven behavioral food-choice adaptations to protein intake.

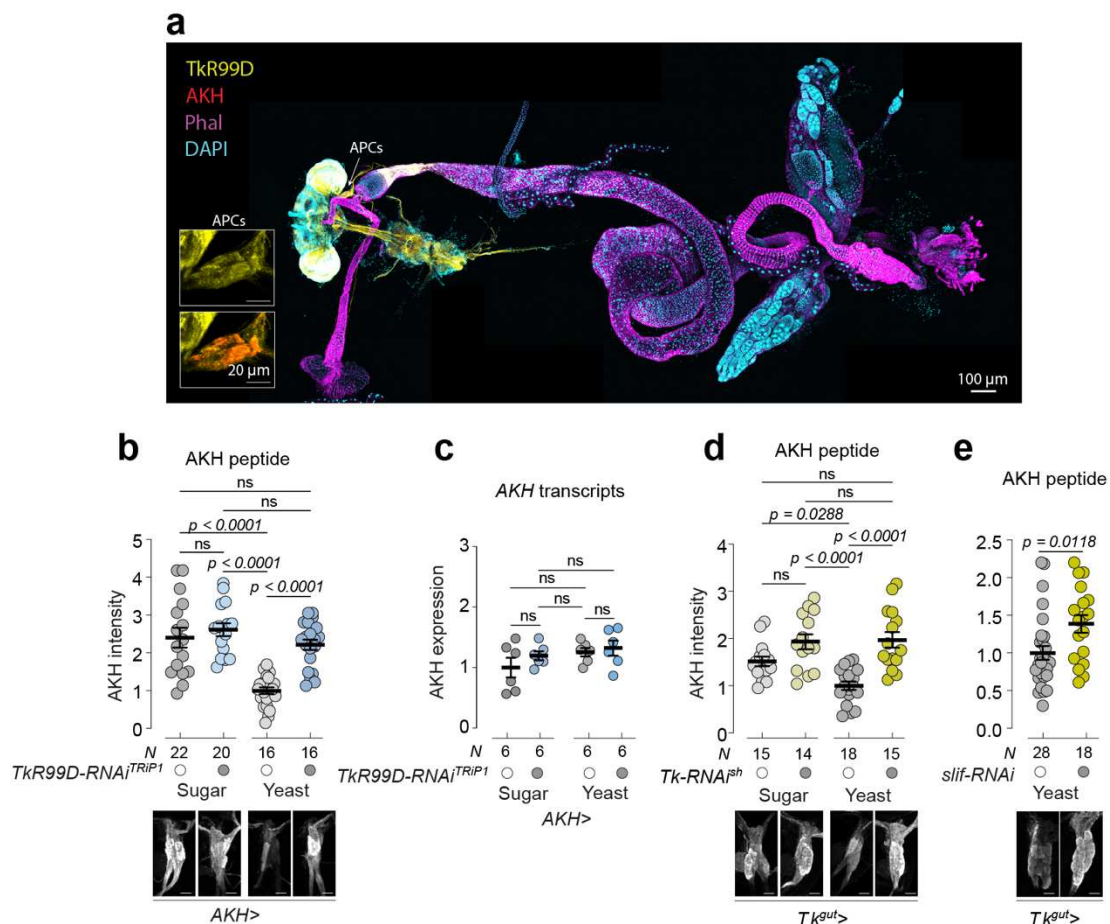


Figure 3. Gut-derived Tk regulates glucagon-like adipokinetic hormone (AKH) signaling in mated females. **a**, Confocal-microscopy image of a single preparation containing the brain and ventral nerve cord, gut, and ovaries, stained for Tk receptor (*TkR99D*>*GFP*, yellow), AKH peptide (red), filamentous actin (Phalloidin, magenta), and DAPI (marking nuclei, blue). AKH-producing cells (APCs) are indicated, with insets showing magnified APCs. Scale bar, 100 μ m (main image) and 20 μ m (inset). **b-e**, Quantitative analyses of AKH peptide levels and *AKH* transcript levels under given conditions. **b-c**, AKH peptide intensity (**b**) in the APCs and whole-body *AKH* transcript levels (**c**) in flies with *TkR99D* silenced in the APCs using *AKH-GAL4* (*AKH*>) and controls, fed on either sugar or yeast diets for 15 h, analyzed by Kruskal-Wallis and Dunn's multiple-comparisons tests. **d**,

Comparison of AKH peptide intensity in flies with knockdown of *Tk* in the EECs ($Tk^{gut}>Tk-RNAi$) and control flies ($Tk^{gut}>$) fed sugar or yeast diets for 15 h, with statistical analysis by one-way ANOVA and Tukey's *post hoc* test. e, AKH peptide levels in animals with knockdown of the amino-acid transporter Slimfast in Tk^+ EECs ($Tk^{gut}>slif-RNAi$) compared to controls ($Tk^{gut}>$) after 15 h yeast feeding, tested with Mann-Whitney U for statistical significance. Sample sizes (N) and *p* values are indicated in each plot. Data are presented as mean \pm SEM. ns, non-significant ($p>0.05$).

In mammals, glucagon is released during periods of fasting and exercise that lead to reduced blood-sugar concentration, triggering the breakdown of energy stores and the repletion of blood sugar. This function is mirrored by the role of AKH in insect energy-store mobilization. Interestingly, protein-rich foods can also trigger glucagon release³¹. Based on this, we hypothesized that *Tk*, released from EECs in response to protein intake, might stimulate the APCs to release AKH. Supporting this notion, we observed reduced intracellular AKH levels in the APCs of animals that had consumed yeast food compared to those on a sugar diet (Fig. 3b). This depletion was not associated with changes in *AKH* transcript levels (Fig. 3c), suggesting that it can be attributed to increased secretion of the AKH peptide in yeast-fed animals. However, this effect was completely abrogated when *Tkr99D* was knocked down in the APCs using *AKH-GAL4 (AKH>)* – yeast feeding did not lead to AKH depletion from the APCs in these animals (Fig. 3b,c). Together our data imply that food high in protein and low in carbohydrates triggers AKH secretion and that *Tkr99D* in the APCs is essential for this effect.

We then investigated whether the release of *Tk* from the midgut is required for the induction of AKH release observed in yeast-fed animals. Phenocopying APC-specific *Tkr99D* knockdown, EEC-specific *Tk* knockdown blocked the yeast-feeding-induced drop in intracellular AKH peptide levels (Fig. 3d). This effect suggests that gut-derived *Tk* promotes AKH secretion through humoral activity in response to the intake of protein-rich food. Given our results indicating that amino-acid sensing mediated by *Slif* in Tk^+ EECs is important for the release of *Tk*, we investigated whether the loss of *Slif* in these cells in the midgut, which leads to *Tk* retention, would also impair AKH release from the APCs. As expected, *slif* knockdown in Tk^+ EECs resulted in greater AKH peptide levels in the APCs after yeast feeding (Fig. 3e). Together, our data imply that food high in protein and low in carbohydrates triggers *Tk* release from EECs through a mechanism involving the amino-acid transporter *Slif*. *Tk* then acts on the APCs through *Tkr99D* to promote AKH secretion.

Tk regulates food choice via effects mediated by glucagon-like signaling

Given that gut-derived *Tk* regulates the release of AKH, a factor that can influence food preferences⁴, we asked whether the observed *Tk*-dependent appetite effects are mediated by AKH. We first investigated whether *Tk* modulates feeding on sugar- versus protein-containing foods through *Tkr99D* in the APCs. Like animals expressing *Tk* knockdown in the EECs, mated adult females with APC-specific *Tkr99D* knockdown displayed diminished sugar consumption over a one-hour period following a 15-hour period of yeast consumption (Fig. 4a). On the other hand, these protein-satiated animals exhibited an increased appetite for protein compared to controls, consuming a greater amount of yeast food (Fig. 4b). In both scenarios, two distinct RNAi lines showed consistent phenotypes (Extended Data Fig. 3a). We validated this elevated sugar consumption through a longer-duration feeding test and confirmed increased sugar-feeding behavior over both medium-term and long-term assays using the automated FLIC and FlyPAD systems (Fig. 4c,d,e and Extended Data Fig. 3,b,c,d,e). We examined whether *Tkr99D* in the APCs influences metabolism and found a minor increase in starvation resistance but no changes in TAG levels in animals with APC-specific *Tkr99D* knockdown under fed conditions (Extended Data Fig. 3f,g), mirroring the effects observed with EEC-specific *Tk* knockdown (Extended Data Fig. 1d). Together with the rapid effects on feeding behavior induced by activation of *Tk* release from the gut, these results collectively suggest that behavior is governed by EEC *Tk* and APC *Tkr99D*.

To ascertain whether AKH mediates the effects of *Tk* or *Tkr99D* loss on feeding, we first assessed the impact of *AKH* knockdown on nutrient-specific appetite. Like gut-specific *Tk* knockdown or APC-targeted *Tkr99D* knockdown, *AKH* knockdown in the APCs led to reduced sugar consumption of yeast-satiated animals (Fig. 4f), and this was not attributable to the RNAi construct alone (Extended Data Fig. 3h). In contrast, these *AKH*-knockdown animals consumed more yeast-based food than

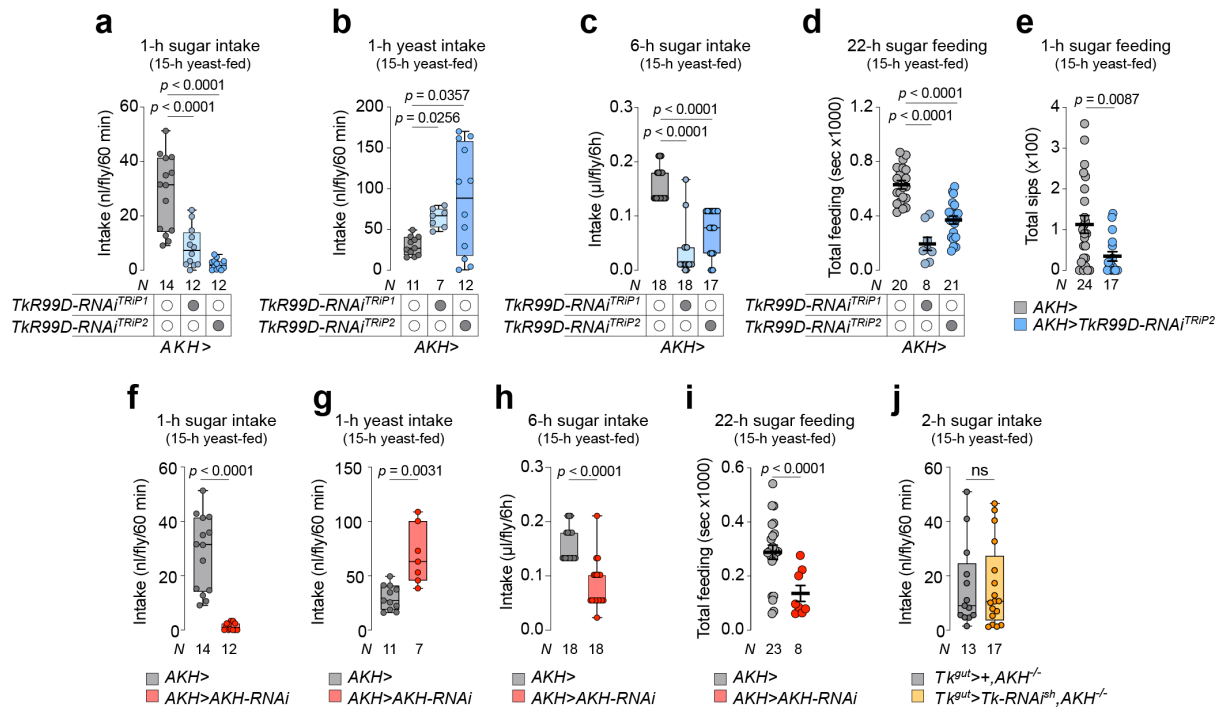


Figure 4. Tk modulates dietary choice through mechanisms driven by glucagon-like signaling pathways in mated females. **a-b**, Short-term nutrient-intake assays for sugar (**a**) and yeast (**b**) of animals with *Tkr99D* silenced in the APCs using the *AKH>* driver compared to controls following a 15-hour yeast pre-feeding period. Statistical analysis using one-way ANOVA with Dunnett's test (**a**), Kruskal-Wallis Dunn test (**b**). **c-d**, Longer-term feeding behavior of animals with *Tkr99D* knockdown in the APCs following a 15-hour yeast pre-feeding period: (**c**) shows a 6-hour sugar-intake assessment with CAFÉ, whereas (**d**) presents 22-hour sugar feeding data obtained using the FLIC (Fly Liquid-food Interaction Counter) system that measures feeding behavior rather than consumption volume. Statistical analysis using Kruskal-Wallis Dunn test (**c**) and one-way ANOVA with Dunnett's test (**d**). **e**, Number of sips of sugar taken in one hour by animals with APC-specific *Tkr99D* knockdown and controls after 15-hour yeast feeding, as measured by the FlyPAD (Fly Proboscis and Activity Detector) assay, showing feeding actions rather than consumption volume. Statistical analysis using Mann-Whitney U. **f-g**, Short-term nutrient-intake CAFÉ assays for sugar (**f**) and yeast (**g**) of animals with *AKH* silenced in the APCs using the *AKH>* driver compared to controls following a 15-hour yeast pre-feeding period. Statistical analysis using Mann-Whitney U test (**f**) and two-tailed unpaired Student's t test (**g**). **h**, Longer-term 6-hour sugar intake of animals with *AKH* knockdown in the APCs following a 15-hour yeast pre-feeding period. CAFÉ assay with statistical analysis using Mann-Whitney U. **i**, 22-hour sugar feeding measured using the flyPAD assay for animals with APC-specific *AKH* knockdown and controls, following a 15-hour yeast pre-feeding period, assay. Statistical analysis using Mann-Whitney U. **j**, CAFÉ assays to assess sugar consumption of *AKH* mutants, with and without gut-specific *Tk* RNAi, following a 15-hour yeast pre-feeding period. Mann-Whitney U was employed for statistical analysis. Sample sizes (N) and *p* values are indicated in each plot. **a, b, c, f, g, h, j**: Box plots indicate minimum, 25th percentile, median, 75th percentile, and maximum values. **d, e, i**: Data are presented as mean ± SEM. ns, non-significant (*p*>0.05).

controls (Fig. 4g). Knockdown of *AKH* also reduced yeast-fed animals' sugar consumption over a longer observation period and decreased the frequency of their sugar-food sips when compared to controls and the RNAi transgene alone (Fig. 4h,i and Extended Data Fig. 3i,j). Thus, *AKH* loss has effects on feeding similar to those seen with gut *Tk* loss or knockdown of the *Tkr99D* in the APCs. To discern whether *AKH* mediates the effects of *Tk* signaling on feeding patterns, we analyzed the ability of gut *Tk* to alter sugar feeding in *AKH*-deficient animals following 15 hours' feeding on yeast diet. Since gut *Tk* knockdown leads to reduced sugar intake (Fig. 1b,f-h), we analyzed food consumption over an extended 2-hour window to detect any variations. In *AKH* mutants, EEC-specific *Tk* knockdown had no effect on sugar intake, suggesting that *AKH* is the primary factor mediating the influence of gut *Tk* on feeding behavior (Fig. 4j). Collectively, our results suggest that gut-derived *Tk*, acting through *Tkr99D* on the

APCs, stimulates AKH release following a protein-rich diet, and AKH inhibits further protein intake and enhances the appetite for sugar.

Protein-rich yeast intake impacts sleep and activity through gut TK and AKH-mediated pathways

Feeding and sleep are interconnected behaviors, with diet exerting a significant influence on sleep and activity patterns. In times of food scarcity, animals often suppress their sleep to prioritize foraging, which increases their activity. Under starvation conditions, the release of AKH suppresses sleep and leads to hyperactivity²⁹, and our recent findings reveal that the gut hormone AstC contributes to this adaptive starvation-induced sleep suppression by modulating AKH³. The macronutrient composition of the diet also seems to influence sleep depth and quality^{32,33}. Although the underlying mechanisms remain largely elusive, recent findings suggest that dietary protein intake may influence arousability – the ease with which stimuli can induce a response during sleep – through peptides released from the gut³⁴. Given that gut *Tk* promotes AKH release in response to protein-rich food intake, we rationalized that protein feeding would suppress sleep and increase activity. When we transitioned animals from a sugar-only diet (commonly used in *Drosophila* sleep studies) to a protein-rich yeast diet, a marked alteration in the sleep and activity patterns of the control group was observed (Fig. 5a,b). As expected, these animals reduced their sleep and increased their activity when fed yeast food compared to sugar-fed conditions, consistent with wakefulness promoted by increased AKH signaling under protein-rich dietary conditions. This increased activity in response to protein feeding was abolished when *Tk* was knocked down in the EECs, suggesting that gut-derived *Tk* drives the effect of dietary protein on sleep and activity regulation (Fig. 5c). Next, we explored whether *Tk* exerts this sleep modulatory effect through *TkR99D* in the APCs, and we probed whether AKH also governs sleep responses to protein feeding. Mirroring the effects of *Tk* knockdown in the gut, *TkR99D* knockdown in the APCs blocked the sleep-suppressing and activity-inducing effect of yeast feeding (Fig. 5d,e,f). Consistent with the effects of *Tk* knockdown in the gut or receptor RNAi in the APCs, animals with loss of *AKH* function also displayed no decrease in sleep or increase in activity when fed yeast compared to sugar-fed conditions (Extended Data Fig. 4a,b,c). Together, these findings indicate that, in environments characterized by diets high in protein and low in carbohydrates, the modulation of AKH release by gut-derived *Tk* orchestrates adaptive feeding, sleep, and activity behaviors. This ensures a balance in nutrient intake and prioritizes feeding over restorative behaviors, such as sleep.

The gut *Tk*-to-AKH axis influences both reproductive output and longevity

Dietary modifications have significant effects on lifespan and fecundity across taxa^{35,36}. A balanced diet generally supports longevity, whereas fecundity in flies is mainly affected by dietary yeast content. Since gut *Tk* is responsive to protein-rich food consumption and modulates dietary choices to maintain nutritional balance, we sought to investigate its potential influence on fecundity and lifespan. We assessed fecundity by quantifying the viable offspring of genetically manipulated females allowed for 24 hours to mate with *w¹¹¹⁸* control males. On a standard diet, which includes both sugar and yeast, reduction of *Tk* expression in the females' EECs with either of two independent RNAi lines resulted in an increased number of offspring (Fig. 6a and Extended Data Fig. 5a). Conversely, females in which *Tk* release was induced through *TrpA1* activation exhibited a marked decrease in offspring number compared to controls. This effect was abolished by concurrent *Tk* knockdown, indicating that the reduction in offspring requires gut-derived *Tk* (Fig. 6b and Extended Data Fig. 5b). Next, we investigated whether, as observed with feeding, this gut-*Tk*-regulated process involves *TkR99D* and AKH in the APCs. Consistent with the consequences of gut *Tk* knockdown, the downregulation of *TkR99D* or *AKH* in these cells resulted in a statistically significant, albeit modest, elevation in fecundity (Fig. 6c and Extended Data Fig. 5c), aligning with reports that diminished AKH signaling increases female fecundity³⁷. Since *TkR99D* is also expressed in the nervous system (Fig. 3a), we examined the effect of pan-neuronal *TkR99D* knockdown on fecundity. Knocking down *TkR99D* in all neurons did not affect the number of offspring produced (Extended Data Fig. 5d), which also suggests that the effects observed with APC knockdown are not due to the presence of the RNAi transgene itself. Our data indicate that gut-derived *Tk* influences the number of offspring a female produces after mating, at least in part by modulating AKH signaling, establishing a link between the yeast-responsive gut factor *Tk*, AKH pathway activity, and fecundity.

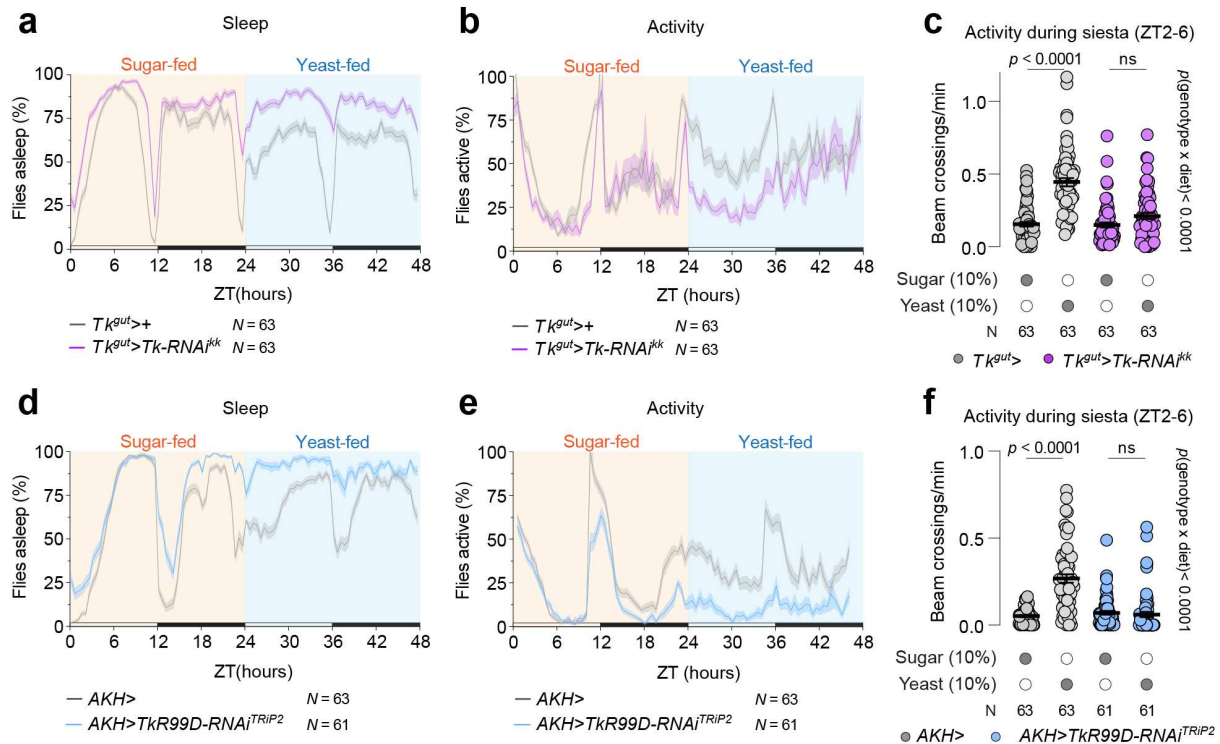


Figure 5. Dietary effects on sleep and activity patterns are influenced by gut *Tk* signaling and AKH pathways in mated females. a-b Sleep (a) and activity (b) profile graphs showing the percentage of flies asleep or active over time for control and gut-specific *Tk*-knockdown flies on sugar and yeast diets. The shaded area represents the standard error of the mean (SEM). c, Quantification of activity during the midday “siesta”, from Zeitgeber Time (ZT) 2 to 6 hours, in flies with *Tk* knockdown in the gut on sugar and yeast diets. Kruskal-Wallis ANOVA with Dunn’s and two-way ANOVA to examine interactions. d-f Sleep (d) and activity (e) profile graphs depicting the percentage of flies asleep or active over time for control groups and flies with knockdown of *TkR99D* in the APCs on sugar and yeast diets. The shaded area represents the standard error of the mean (SEM). f, Quantitative analysis of activity during siesta, spanning ZT 2 to 6 hours, in flies with *TkR99D* knockdown in the APCs, maintained on sugar and yeast diets. Kruskal-Wallis ANOVA with Dunn’s and two-way ANOVA to examine interactions. Sample sizes (N) and *p* values are indicated in each plot. Data are presented as mean \pm SEM. ns, non-significant ($p > 0.05$).

Dietary yeast concentration influences the lifespan of *Drosophila*, with increasing levels reducing their longevity^{38,39}. Given that gut *Tk* is secreted in response to dietary yeast, we explored whether *Tk* might be involved in determining longevity. Silencing gut *Tk* via either of two independent RNAi lines resulted in lifespan extension on both the 10%- and 20%-yeast diets (Fig. 6d). Conversely, to mimic conditions of high protein consumption for *Tk* signaling, we induced *Tk* release via *TrpA1* expression in EECs, which led to decreased longevity on both diets, with a more pronounced effect observed on the 10%-yeast diet (a 4.4-day reduction) than on the higher-yeast medium (a 2.1-day reduction). This difference may arise because the Tk^+ EECs are presumably already more active on the 20%-yeast diet. Although the calcium activity of Tk^+ EECs was not elevated on a 20%-yeast diet compared to a 10%-yeast diet, the *Tk* peptide levels in the EECs were reduced, indicating that there may be an increased release of *Tk* from the gut (Extended Data Fig. 5e). On the 10%-yeast diet, the negative impact on lifespan of activating the Tk^+ EECs was partially abrogated by concurrent *Tk* knockdown, suggesting that the lifespan-shortening effect is partially driven by *Tk* release. Tk^+ EECs also produce NPF, which responds to dietary sugar^{4,12}, and this second factor may give rise to a confounding effect in animals fed the 10%-yeast diet, in which sugar and yeast are relatively more balanced, potentially triggering greater NPF release. Consistent with this view, NPF⁺ EECs exhibited higher calcium activity on the 10%-yeast diet compared to the richer medium (Extended Data Fig. 5f), suggesting that NPF release may indeed contribute to the phenotype observed on the 10%-yeast diet, which is relatively richer in sugar compared to the 20%-yeast diet. In contrast, on the 20%-yeast diet,

also rules out the possibility that the transgene itself causes effects independent of AKH. Collectively, our results demonstrate that gut-secreted Tk modulates behavioral adaptations in food selection and sleep following the consumption of protein-rich yeast food, and it also influences lifespan – effects which are all mediated by the regulation of the glucagon-like hormone AKH.

Discussion

Feeding behavior is influenced by diverse internal and external cues and regulated by a complex interplay of hormones that control appetite. Beyond matching the animal's energy intake with its needs by simply eating more or less, the balance between macronutrient types must be maintained through consumption of specific nutrients. Strong evidence from many animals, including humans, show that nutrient-specific appetites drive food selection according to internal macronutrient requirements⁴⁰. Although many hormones are known to regulate appetite in general, the endocrine mechanisms underlying the regulation of nutrient-specific hungers are not well understood. Protein intake induces a strong satiety response compared to fat and carbohydrate, and gut-derived hormones are postulated to mediate this protein-induced satiety response⁴¹. We present evidence that the EEC-derived hormone Tachykinin is indeed such a regulator of selective appetite that induces protein-specific satiety in flies. Our work indicates that, upon protein intake, Tk is secreted by EECs and, via its regulation of AKH signaling, mediates the suppression of appetite for protein-rich food while simultaneously promoting a preference for dietary sugars. Like Tk, its mammalian ortholog Substance P is also expressed in EECs^{42,43}, but the function of EEC-derived Tk/Substance P remains poorly defined. Our findings here suggest that an examination of the role of EEC-derived Tk/Substance P in appetite regulation would be an interesting endeavor.

Previous studies have demonstrated that EECs of both flies and humans can sense nutrients including sugars, amino acids, and fatty acids, triggering the release of hormones that modulate systemic metabolism and influence behaviors including feeding^{3,4,12,14,44}. EECs of the mammalian intestine secrete GLP-1 in response to the ingestion of carbohydrates and lipids, and this signal suppresses appetite and decreases food intake while simultaneously potentiating glucose-stimulated insulin secretion and reducing glucagon release. Similarly, we have found that gut-derived NPF, the *Drosophila* homolog of mammalian Peptide YY (PYY), is secreted by EECs in response to carbohydrate consumption and acts as a sugar-specific satiety hormone⁴. NPF also inhibits postprandial glucagon-like AKH signaling and enhances insulin secretion, effects analogous with those of mammalian GLP-1¹². Here, we show that intake of protein-rich food activates Tk⁺ EECs through a mechanism requiring the conserved amino-acid transporter Slif (orthologous with mammalian SLC7A-family amino-acid transporters). Amino-acid detection leads to the release of Tk, which then acts as a protein-specific satiety hormone. In mammals, Taste Receptor Type 1 Member 1 (TAS1R1) and Member 3 (TAS1R3), expressed in certain EECs, are known to detect specific amino acids and to influence these cells' cholecystokinin secretion⁴⁵. Solute Carrier Family 7 (SLC7A) cationic-amino-acid transporters are also expressed in the mammalian intestine⁴⁶. However, the mechanisms by which amino-acid sensing in EECs translates into the secretion of hormones that regulate protein-specific appetite in humans remain elusive⁴⁰. Since TAS1R1/3 are G protein-coupled receptors (GPCRs) that detect extracellular amino acids and regulate intracellular pathways through second-messenger signaling, whereas Slimfast is a transporter that permits amino acids to interact directly with intracellular pathways, including Target of Rapamycin (TOR), a number of diverse mechanisms are likely involved. Future investigations should decipher the role of SLC7-family amino-acid transporters in linking consumed amino acids to EEC-mediated secretion of hormones that govern mammalian feeding behaviors.

Our data suggest that dietary protein intake, like sugar ingestion, influences the homeostatic regulation of food preference and indicate that EEC-derived Tk governs this feeding behavior. We propose that EEC-derived Tk and NPF function antagonistically to balance protein- and sugar-specific appetites, thereby balancing consumption of these nutrients with the needs of the animal. Consistent with this, our findings suggest that nutrient-specific sensing mechanisms permit Tk⁺ EECs to respond to dietary protein while allowing dietary sugar to stimulate NPF⁺ EECs^{4,14}. Gut-derived Tk and NPF converge on the APCs to regulate dietary choice via their opposing effects on AKH release. The best-studied role of AKH, acting like mammalian glucagon, is to induce lipolysis and elevate blood

(hemolymph) sugar levels. We recently showed that AKH regulates feeding preferences as well, to coordinate energy intake with mobilization^{3,4,14}. Gut-derived Tk stimulates AKH release following protein intake, which promotes protein satiety, whereas gut-derived NPF inhibits AKH secretion after sugar intake, thereby promoting sugar satiety. Studies by others indicate that dietary protein also induces the EEC-mediated release of the hormones CCHamide-1 and Dh31, which influence behaviors including arousal³⁴ and the prioritization between the mutually exclusive behaviors of mating and feeding¹¹. Our study advances the understanding of protein-responsive EEC-derived satiety signals in food-choice regulation.

FGF21 is a protein-specific hunger hormone produced by the mammalian liver that acts on the hypothalamus to increase protein intake and reduce sugar consumption^{7,47}. Although research has demonstrated that protein intake can increase the levels of gut hormones including GLP-1 and PYY, which inhibit appetite⁴⁵, hormones that signal protein-specific satiety have not been reported. The protein leverage hypothesis proposes that protein consumption is prioritized over other dietary components, with the satiating effects of protein exceeding those of carbohydrates and fats. In modern calorie-rich, protein-poor diets, this can lead to overconsumption and obesity^{5,6}. Our study suggests that gut-derived Tk functions as a protein-satiety hormone, which may help explain the endocrine mechanisms underlying this phenomenon.

Dietary restriction, particularly the limitation of protein intake, is one of the main factors that extends lifespan across species^{48,49}. Protein restriction induces hepatic FGF21 release, which has been shown to prolong lifespan in mice⁵⁰. In contrast, we observed that EEC-derived Tk, stimulated by protein consumption, affects lifespan in the opposite direction – high levels (corresponding to a high protein intake) lead to a reduction in lifespan, whereas its inhibition (mimicking low protein consumption) promotes longevity. Our work here indicates that gut Tk may mediate the link between high protein intake and shortened lifespan. Intriguingly, naked mole rats, renowned for their slow aging and exceptionally long lifespans, exhibit no or very low neuronal Tk/Substance P signaling⁵¹. Investigating the potential connection between the absence of Tk/Substance P signaling and increased lifespan represents an interesting direction for future research. Our findings imply that the extended lifespan of flies with EEC-specific Tk deficiency does not entail a trade-off with fecundity under the tested laboratory conditions, indicating that it does not compromise overall fitness.

The role of the gut in mediating the beneficial effects of dietary restriction on lifespan is becoming more salient⁵², but the underlying mechanisms remain unclear, and the impacts of gut-derived hormones on aging have not previously been reported. Given the surge in popularity of metabolic-disorder therapies based on gut hormones such as GLP-1, an understanding of how these hormones influence overall healthspan and longevity is becoming more necessary. We show here that the effect of EEC-derived Tk on lifespan is dependent on AKH, since modulation of gut Tk in *Akh* mutants has no effect on lifespan. One possible explanation of this observation might be that gut Tk, via AKH potentiation, tends to reduce lifespan by altering the balance between protein and sugar intake, upregulating the former at the expense of the latter, which has been shown to influence aging in diverse organisms^{53,54}. Alternatively, gut Tk and AKH may influence lifespan by modulating systemic metabolism and stress tolerance, factors that are also known to affect aging^{53,55}. Further research is needed to decipher the molecular and cellular pathways through which gut Tk and AKH affect longevity.

In conclusion, our study contributes to the understanding of nutrient-specific satiety signals and the role of EEC-derived hormones in regulating food choices and lifespan. These insights have significant implications for understanding the mechanisms of nutrient sensing and appetite regulation, which may potentially be targeted in preventive or therapeutic strategies for metabolic disorders and aging.

Methods

Fly Stocks and Maintenance

Animals were raised on a standard laboratory medium (82 g/L cornmeal, 60 g/L sucrose, 34 g/L yeast, 8 g/L agar, 4.8 mL/L propionic acid, and 1.6 g/L methyl-4-hydroxybenzoate preservative) at 25 °C, 60% humidity, and 12-h light/dark cycle. Before experiments, adult males and females were transferred together to an adult-optimized diet lacking cornmeal (90 g/L sucrose, 80 g/L yeast, 10 g/L agar, 5 mL/L propionic acid, and 15 mL/L of 10% methyl-4-hydroxybenzoate in ethanol)⁵⁶ for 6-7 days. Male and

female animals were separated one day before experiments. Animals were transferred to fresh vials of food every three days. Fly lines are listed in Supplementary Table 1. To minimize genetic-background effects, all GAL4 and GAL80 lines were backcrossed for several generations into the same non-isogenized but genetically well-regimented background population before they were used to drive RNAi lines or crossed to this same w^{1118} as a control.

Feeding Assays

Prior to feeding assays, mated females were protein- or sugar-sated during a 15-hour feeding on yeast medium (10% yeast alone in 1% agar) or sugar medium (10% sucrose alone in 1% agar). All food-intake experiments were performed during subjective breakfast time, beginning at ZT1 (one hour after lights-on). Short-term consumption was assessed using a one-hour dye-based feeding assay^{36,57}. Flies were transferred without anesthesia to adult medium containing 0.5% erioglaucline (blue) dye (Sigma-Aldrich #861146) and allowed to feed for 60 minutes (or 120 minutes for Fig. 4j). In parallel, similar flies were transferred to undyed food for measurement of the baseline absorbance of fly lysates. Lysate samples were prepared by homogenizing single flies in 100 μ L of phosphate buffer, pH 7.5, using a TissueLyser LT (Qiagen) bead mill with 5-mm stainless-steel beads (Qiagen, #69989). These lysates were clarified by a five-minute centrifugation at 16,000 g, after which 50 μ L of supernatant was loaded into a 384-well plate. Sample absorbance was measured at 629 nm on an EnSight multi-mode plate reader (PerkinElmer). A standard curve for erioglaucline was used to convert absorbance values to food-consumption amounts.

Longer-term food intake was monitored using the capillary feeding (CAFÉ) assay¹⁵. For single-fly consumption assays, a 5- μ L capillary tube (Hirschmann, #9000105), filled with 10% sucrose in water containing preservatives (0.1% propionic acid and 0.1% methyl-4-hydroxybenzoate), was inserted through a hole in the lid of a 2-mL Eppendorf tube. Individual flies were briefly cold-anaesthetized for transfer into these tubes, and similar tubes containing no flies were used as controls for evaporation. The prepared tubes were then kept inside a moist chamber within a standard fly incubator, and the movement of the liquid-medium meniscus within the capillary was recorded over time.

For automated longer-term recording of feeding behaviors, the FLIC (Fly Liquid-Food Interaction Counter) apparatus was used to detect feeding events over 6-24 hours¹⁶. *Drosophila* Feeding Monitors (DFMs; Sable Systems, US) were maintained in an incubator (25 °C; 70% humidity, 12:12-hour light/dark cycle). The food tank of each DFM was filled before experiments with a solution of 10% sucrose in water. Single animals were placed in each of the 12 DFM chambers. Feeding behaviors were analysed in *R Studio* using the published FLIC package, available at https://github.com/PletcherLab/FLIC_R_Code.

The flyPAD apparatus¹⁷ was also used for sugar and yeast feeding in a two-choice behavioral assay. A 3- μ L droplet of medium containing either 10% sucrose or 10% yeast in 1% agar was loaded into the food pedestals of each flyPAD. Flies were briefly cold-immobilized and transferred into the flyPAD behavioral arenas. After several minutes' acclimation, each fly's behavior was recorded using the developer's software within the Bonsai data-stream-processing environment. Analysis was performed using the developer's software, which is available at <https://www.flypad.pt>.

Immunohistochemistry and confocal imaging

To visualize EEC activity, we utilized the CaLexA (calcium-dependent nuclear import of LexA) system, in which calcium concentration is reflected in GFP expression. Because of the relatively long perdurance of GFP, its abundance can be measured after the fact as a reporter of integrated recent calcium-signaling activity. Co-expressed calcium-independent tdTomato acts as a ratiometric control for normalizing GAL4 expression in each cell. Animals expressing *UAS-CaLexA-GFP* and *UAS-tdTomato* in the Tk-producing EECs under the control of *Tk^{gut}-GAL4* were fed for the indicated interval with either 10% yeast, 10% sucrose, or Bacto peptone (ThermoFisher, #211677), after which their guts or APCs were dissected in cold PBS and fixed in 4% formaldehyde in PBS for 1 hour (guts) or 20 minutes (APCs) at room temperature with agitation. Tissues were washed three times, each time for 20 minutes, with PBST (PBS+0.1% Triton X-100) and blocked with 5% normal goat serum in PBST for one hour, all at room temperature with agitation. Tissues were stained with mouse anti-GFP (ThermoFisher, #A11120; 1:500), rat anti-mCherry (for the mCherry derivative tdTomato;

ThermoFisher, #M11217; 1:1000), and rabbit anti-Tk or rabbit anti-AKH (both kind gifts from Jan Veenstra; 1:1000) overnight at 4 °C with agitation.

Tissues were then washed again three times in PBST before being incubated overnight at 4 °C in secondary-antibody solution [Alexa Fluor 488-conjugated goat anti-mouse (ThermoFisher, #A32723); Alexa Fluor 555-conjugated goat anti-rat (ThermoFisher, #A21434); Alexa Fluor 647-conjugated goat anti-rabbit (ThermoFisher, #A11012); and Alexa Fluor 647-conjugated goat anti-rabbit (ThermoFisher, #32733) all diluted 1:500 in PBST]. Tissues were washed three further times and mounted in ProLong Glass (Invitrogen, #36984, for stains including Alexa Fluor 647, which is quenched by Vectashield⁵⁸), Fluoroshield with DAPI (Sigma, #F6057), or Vectashield (Vector Laboratories, #H-1200) anti-fade mountants either on slides coated with poly-L-lysine (Sigma, #P8920) and sealed using a 0.12-mm spacer (Grace Bio-Labs, #654006) or on 35-mm glass-bottom dishes (MatTek Corporation, MA, USA, # P35G-0-10-C) sealed with a 0.1-mm glass cover slip. Slides were imaged using a Zeiss LSM-900 confocal microscope and the Zen acquisition software. All samples that were quantitatively compared to one another were prepared simultaneously with the same staining preparations and imaged with the same hardware and software settings. Image analysis was performed using the open-source program ImageJ and a MatLAB script⁴ to automate the process of identifying cells in confocal image stacks, quantifying the fluorescence signal in each channel, and subtracting the local background intensity. CaLexA signal was normalized to the tdTomato intensity – the reported data points represent the ratio of GFP to tdTomato within each cell to control for variation in GAL4 activity.

Luciferase activity measurement

Midguts from females expressing *UAS-CaLexA-Luciferase* in the Tk-producing EECs were excised and placed into lysis buffer (Promega, #E2920), with luciferase activity measured as previously described⁴. Four midguts per replicate were homogenized in 50 µL of lysis buffer within 2-mL round-bottom Eppendorf tubes using a TissueLyser LT (Qiagen) and 5-mm stainless steel beads (Qiagen, #69989). The lysates were clarified by centrifugation at 21,000 g for 5 minutes, after which supernatants were transferred into fresh tubes and centrifuged a second time. A 10-µL aliquot of this twice-cleared supernatant was dispensed into 384-well plate, to which an equal volume of “Steady Glo” reagent (Promega, #E2510) was added. The plate was then incubated at room temperature for 15 minutes, after which the luciferase activity was measured using the luminescence setting on an EnSight multi-mode plate reader (PerkinElmer).

Calcium Imaging

An *ex-vivo* midgut setup was prepared for transient calcium imaging using *Tk::2A::GAL4* to drive the expression of GCaMP6s²¹ in Tk⁺ EECs. Midguts were dissected from the respective genotypes in a modified Schneider's medium, specifically formulated for adult *Drosophila* tissues⁵⁹. The dissected midguts were then carefully mounted on a small bed of low-melting-temperature agarose (Merck, #A9414) laid on a glass-bottomed dish (MatTek). To immobilize the tissues, a droplet of 0.5% low-melting-temperature agarose was applied atop each midgut. After the agar solidified, 100 µL of the modified Schneider's medium was added to cover the tissue. Live imaging of these samples was performed for one hour using a Zeiss LSM-900 microscope with a 20x/0.8 NA objective lens. GCaMP was excited with a 488-nm laser line. The imaging aimed to compare calcium activity in particular midgut regions when animals were fed yeast versus sugar for 2 h following 15-h starvation before imaging. The intensity over time was quantified for each EEC in the midgut using a custom ImageJ⁶⁰ macro.

Transcript Analysis using qPCR

For each condition, six replicates, each containing five nervous systems or midguts, were homogenized in 2-mL Eppendorf tubes containing lysis buffer from the RNA-prep kit with 1% beta-mercaptoethanol using a TissueLyser LT bead mill (Qiagen) and 5-mm stainless steel beads (Qiagen #69989). Total RNA was purified using the NucleoSpin RNA kit (Macherey-Nagel, #740955). Complementary DNA was prepared using the High-Capacity cDNA Synthesis kit (Applied Biosystems, #4368814). RealQ Plus 2x SYBR Green Master Mix (Ampliqon, #A324402) was used in qPCR reactions on a QuantStudio 5 (Applied Biosystems) machine. The housekeeping gene *Rp49* was used to normalize gene expression values. The oligos used are listed in Supplementary Table 2.

Metabolite measurements

Established protocols were used to measure whole-body levels of triacylglycerides (TAG)⁶¹. Ten samples containing 4 flies each were homogenized in PBS containing 0.05% Tween-20 (Sigma #1379) in a TissueLyser LT (Qiagen) bead mill with 5-mm stainless-steel beads. TAGs were hydrolyzed using Triglyceride Reagent (Sigma, #T2449) to liberate the glycerol backbone, and the amount of this compound was determined using Free Glycerol Reagent (Sigma, #F6428) in a colorimetric assay. The absorbance of each reacted sample at 540 nm was measured in a 384-well plate using an EnSight multimode plate reader (PerkinElmer); standard curves were used to calculate TAG concentrations. Protein levels were measured in the same extracts using a bicinchoninic-acid (BCA) assay [bicinchoninic acid solution, Sigma, #B9643; copper sulfate solution, #C2284, and bovine serum albumin (BSA) protein standards, #P0914], with absorbance measured at 562 nm. Standard curves were used to calculate the protein concentration in each fly extract, and TAG levels were normalized to these values to control for variability in the number and size of animals – TAG data are reported as micrograms of TAG per milligram of protein.

Starvation-survival assay

Animals were transferred to vials containing 1% agar in water (starvation medium), fifteen per vial. Vials were placed in a 25 °C incubator, and the number of dead animals in each vial was recorded every 8 hours until none remained alive. The 50%-survival time was calculated by linearly interpolating between the measurements flanking 50% survival.

Longevity assay

Mated females were transferred to vials containing either 10% or 20% yeast medium (consisting of 10% or 20% yeast, 10% sucrose, and 1% agar in water. At least four vials per genotype with twenty flies per vial was used. The number of surviving flies was recorded daily at the same time, continuing until no flies remained alive. To ensure optimal conditions, flies were transferred to fresh medium every 96 hours.

Fecundity assay

Ten female flies were allowed to mate with five w1118 males for 24 hours at 25 °C in vials containing adult-optimized diet described above. The mated females were then anesthetized using CO₂ and transferred to fresh vials for one day of acclimation. The following day, flies were transferred to fresh experimental vials. The flies were transferred to fresh adult medium vials every 24 hours, at the same timepoint each day. The number of pupae present in each vial was recorded after a few days. The experiment was continued until the flies no longer laid eggs or laid very few.

Sleep and activity assays

Sleep and activity patterns were monitored using the *Drosophila* Activity Monitoring System (TriKinetics, Waltham, MA). Six-to-seven-day-old flies were transferred under CO₂ anesthesia to glass tubes stoppered at one end with a foam plug and sealed at the other with a removable 250- μ L PCR tube containing 90 μ L of either 5% sucrose or 5% yeast in 1% agarose/water, supplemented with 0.5% propionic acid and 0.15% methyl-4-hydroxybenzoate, and locomotor activity was recorded beginning at lights-on. After 24 hours, the food tubes were replaced with fresh food. Intervals of at least 5 minutes without detected activity were classified as “sleep.”

Statistics

All statistics were computed using the Prism analysis package (version 9; GraphPad). Survival curves were analyzed using Kaplan-Meier log-rank tests or Gehan-Breslow-Wilcoxon tests. Other data were checked for normality before determinations of significance were made. Pairwise comparisons between normal data were made using two-tailed unpaired Student's t-tests, and multiple normally distributed samples were compared using one-way ANOVA with Tukey's multiple-comparisons tests. Two-tailed unpaired Mann-Whitney U tests or one-way Kruskal-Wallis ANOVAs followed by Dunn's multiple-comparisons tests were used to compare non-normal data. Two-way ANOVA was performed to examine interactions. Bar plots of normal data indicate the mean plus/minus the standard error of the mean

(SEM), and for non-normal data the median and 95% confidence interval are indicated. Preference indices for option A over option B were calculated as “(amount of A – amount of B)/(amount of A + amount of B)”.

Data Availability

Reasonable data requests will be fulfilled by the lead author.

Code Availability

The scripts used for analyzing images and locomotion data in this study can be accessed publicly at <https://doi.org/10.5281/zenodo.6641933> and <https://doi.org/10.5281/zenodo.6641957> as described⁴.

Acknowledgements

This work was supported by Novo Nordisk Foundation grant NNF19OC0054632 and Lundbeck Foundation grant 2019-772 to KR. TK and KVH were supported by funding from the Danish Independent Research Council – Natural Sciences (9064-00009B) to KVH. The Zeiss LSM 900 confocal microscope and the PerkinElmer EnSight plate reader were purchased with generous grants from the Carlsberg Foundation (no. CF19-0353 and CF17-0615, respectively) to K.R.

Author contributions

NA and KR conceived and designed the study. NA, OK, AM, TK, KVH, SN, MJT, and KR designed, performed, and analyzed experiments. MJT and KR wrote the manuscript.

Competing interests

Authors declare that no competing interests exist.

References

- 1 Carreiro, A. L. *et al.* The Macronutrients, Appetite, and Energy Intake. *Annual review of nutrition* **36**, 73-103 (2016). <https://doi.org/10.1146/annurev-nutr-121415-112624>
- 2 Munch, D., Ezra-Nevo, G., Francisco, A. P., Tastekin, I. & Ribeiro, C. Nutrient homeostasis - translating internal states to behavior. *Curr Opin Neurobiol* **60**, 67-75 (2020). <https://doi.org/10.1016/j.conb.2019.10.004>
- 3 Kubrak, O. *et al.* The gut hormone Allatostatin C/Somatostatin regulates food intake and metabolic homeostasis under nutrient stress. *Nature communications* **13**, 692 (2022). <https://doi.org/10.1038/s41467-022-28268-x>
- 4 Malita, A. *et al.* A gut-derived hormone suppresses sugar appetite and regulates food choice in *Drosophila*. *Nat Metab* **4**, 1532-1550 (2022). <https://doi.org/10.1038/s42255-022-00672-z>
- 5 Khan, M. S. *et al.* Protein Appetite at the Interface between Nutrient Sensing and Physiological Homeostasis. *Nutrients* **13** (2021). <https://doi.org/10.3390/nu13114103>
- 6 Simpson, S. J. & Raubenheimer, D. Obesity: the protein leverage hypothesis. *Obes Rev* **6**, 133-142 (2005). <https://doi.org/10.1111/j.1467-789X.2005.00178.x>
- 7 Hill, C. M. *et al.* FGF21 Signals Protein Status to the Brain and Adaptively Regulates Food Choice and Metabolism. *Cell reports* **27**, 2934-2947 e2933 (2019). <https://doi.org/10.1016/j.celrep.2019.05.022>
- 8 Kosakamoto, H. *et al.* Sensing of the non-essential amino acid tyrosine governs the response to protein restriction in *Drosophila*. *Nat Metab* **4**, 944-959 (2022). <https://doi.org/10.1038/s42255-022-00608-7>
- 9 Cai, X. T. *et al.* Gut cytokines modulate olfaction through metabolic reprogramming of glia. *Nature* **596**, 97-102 (2021). <https://doi.org/10.1038/s41586-021-03756-0>
- 10 Kim, B. *et al.* Response of the microbiome-gut-brain axis in *Drosophila* to amino acid deficit. *Nature* **593**, 570-574 (2021). <https://doi.org/10.1038/s41586-021-03522-2>
- 11 Lin, H. H. *et al.* A nutrient-specific gut hormone arbitrates between courtship and feeding. *Nature* (2022). <https://doi.org/10.1038/s41586-022-04408-7>

- 12 Yoshinari, Y. *et al.* The sugar-responsive enteroendocrine neuropeptide F regulates lipid metabolism through glucagon-like and insulin-like hormones in *Drosophila melanogaster*. *Nature communications* **12**, 4818 (2021). <https://doi.org:10.1038/s41467-021-25146-w>
- 13 Finer, N. Future directions in obesity pharmacotherapy. *Eur J Intern Med* **93**, 13-20 (2021). <https://doi.org:10.1016/j.ejim.2021.04.024>
- 14 Park, J. H. *et al.* A subset of enteroendocrine cells is activated by amino acids in the *Drosophila* midgut. *FEBS Lett* **590**, 493-500 (2016). <https://doi.org:10.1002/1873-3468.12073>
- 15 Ja, W. W. *et al.* Prandiology of *Drosophila* and the CAFE assay. *Proc Natl Acad Sci U S A* **104**, 8253-8256 (2007). <https://doi.org:10.1073/pnas.0702726104>
- 16 Ro, J., Harvanek, Z. M. & Pletcher, S. D. FLIC: high-throughput, continuous analysis of feeding behaviors in *Drosophila*. *PLoS One* **9**, e101107 (2014). <https://doi.org:10.1371/journal.pone.0101107>
- 17 Itskov, P. M. *et al.* Automated monitoring and quantitative analysis of feeding behaviour in *Drosophila*. *Nature communications* **5**, 4560 (2014). <https://doi.org:10.1038/ncomms5560>
- 18 Hamada, F. N. *et al.* An internal thermal sensor controlling temperature preference in *Drosophila*. *Nature* **454**, 217-220 (2008). <https://doi.org:10.1038/nature07001>
- 19 Masuyama, K., Zhang, Y., Rao, Y. & Wang, J. W. Mapping neural circuits with activity-dependent nuclear import of a transcription factor. *Journal of neurogenetics* **26**, 89-102 (2012). <https://doi.org:10.3109/01677063.2011.642910>
- 20 Song, W., Veenstra, J. A. & Perrimon, N. Control of lipid metabolism by tachykinin in *Drosophila*. *Cell reports* **9**, 40-47 (2014). <https://doi.org:10.1016/j.celrep.2014.08.060>
- 21 Chen, T. W. *et al.* Ultrasensitive fluorescent proteins for imaging neuronal activity. *Nature* **499**, 295-300 (2013). <https://doi.org:10.1038/nature12354>
- 22 Guo, F., Chen, X. & Rosbash, M. Temporal calcium profiling of specific circadian neurons in freely moving flies. *Proc Natl Acad Sci U S A* **114**, E8780-E8787 (2017). <https://doi.org:10.1073/pnas.1706608114>
- 23 Li, H. *et al.* Fly Cell Atlas: A single-nucleus transcriptomic atlas of the adult fruit fly. *Science* **375**, eabk2432 (2022). <https://doi.org:10.1126/science.abk2432>
- 24 Colombani, J. *et al.* A nutrient sensor mechanism controls *Drosophila* growth. *Cell* **114**, 739-749 (2003). <https://doi.org:S009286740300713X> [pii]
- 10.1016/S0092-8674(03)00713-X
- 25 Guo, X. *et al.* The Cellular Diversity and Transcription Factor Code of *Drosophila* Enteroendocrine Cells. *Cell reports* **29**, 4172-4185 e4175 (2019). <https://doi.org:10.1016/j.celrep.2019.11.048>
- 26 Hung, R. J. *et al.* A cell atlas of the adult *Drosophila* midgut. *Proc Natl Acad Sci U S A* **117**, 1514-1523 (2020). <https://doi.org:10.1073/pnas.1916820117>
- 27 Inagaki, H. K., Panse, K. M. & Anderson, D. J. Independent, reciprocal neuromodulatory control of sweet and bitter taste sensitivity during starvation in *Drosophila*. *Neuron* **84**, 806-820 (2014). <https://doi.org:10.1016/j.neuron.2014.09.032>
- 28 Koyama, T. *et al.* A nutrient-responsive hormonal circuit mediates an inter-tissue program regulating metabolic homeostasis in adult *Drosophila*. *Nature communications* **12**, 5178 (2021). <https://doi.org:10.1038/s41467-021-25445-2>
- 29 Lee, G. & Park, J. H. Hemolymph sugar homeostasis and starvation-induced hyperactivity affected by genetic manipulations of the adipokinetic hormone-encoding gene in *Drosophila melanogaster*. *Genetics* **167**, 311-323 (2004).
- 30 Yu, Y. *et al.* Regulation of starvation-induced hyperactivity by insulin and glucagon signaling in adult *Drosophila*. *Elife* **5** (2016). <https://doi.org:10.7554/eLife.15693>
- 31 Ang, T., Bruce, C. R. & Kowalski, G. M. Postprandial Aminogenic Insulin and Glucagon Secretion Can Stimulate Glucose Flux in Humans. *Diabetes* **68**, 939-946 (2019). <https://doi.org:10.2337/db18-1138>

- 32 Peuhkuri, K., Sihvola, N. & Korpela, R. Diet promotes sleep duration and quality. *Nutr Res* **32**, 309-319 (2012). <https://doi.org:10.1016/j.nutres.2012.03.009>
- 33 Murphy, K. R. *et al.* Postprandial sleep mechanics in *Drosophila*. *Elife* **5** (2016). <https://doi.org:10.7554/eLife.19334>
- 34 Titos, I. *et al.* A gut-secreted peptide suppresses arousability from sleep. *Cell* **186**, 2273-2274 (2023). <https://doi.org:10.1016/j.cell.2023.04.005>
- 35 Piper, M. D. W. *et al.* Dietary restriction and lifespan: adaptive reallocation or somatic sacrifice? *FEBS J* **290**, 1725-1734 (2023). <https://doi.org:10.1111/febs.16463>
- 36 Skorupa, D. A., Dervisefendic, A., Zwiener, J. & Pletcher, S. D. Dietary composition specifies consumption, obesity, and lifespan in *Drosophila melanogaster*. *Aging Cell* **7**, 478-490 (2008). <https://doi.org:10.1111/j.1474-9726.2008.00400.x>
- 37 Wat, L. W., Chowdhury, Z. S., Millington, J. W., Biswas, P. & Rideout, E. J. Sex determination gene transformer regulates the male-female difference in *Drosophila* fat storage via the adipokinetic hormone pathway. *Elife* **10** (2021). <https://doi.org:10.7554/eLife.72350>
- 38 Mair, W., Piper, M. D. & Partridge, L. Calories do not explain extension of life span by dietary restriction in *Drosophila*. *PLoS Biol* **3**, e223 (2005). <https://doi.org:10.1371/journal.pbio.0030223>
- 39 Bass, T. M. *et al.* Optimization of dietary restriction protocols in *Drosophila*. *J Gerontol A Biol Sci Med Sci* **62**, 1071-1081 (2007). <https://doi.org:10.1093/gerona/62.10.1071>
- 40 Hopkins, M. & Blundell, J. E. in *Appetite and Food Intake: Central Control* (ed R. B. S. Harris) 259-276 (2017).
- 41 Morrison, C. D. & Laeger, T. Protein-dependent regulation of feeding and metabolism. *Trends Endocrinol Metab* **26**, 256-262 (2015). <https://doi.org:10.1016/j.tem.2015.02.008>
- 42 Aiken, K. D. & Roth, K. A. Temporal differentiation and migration of substance P, serotonin, and secretin immunoreactive enteroendocrine cells in the mouse proximal small intestine. *Dev Dyn* **194**, 303-310 (1992). <https://doi.org:10.1002/aja.1001940406>
- 43 Bai, L. *et al.* Enteroendocrine cell types that drive food reward and aversion. *Elife* **11** (2022). <https://doi.org:10.7554/eLife.74964>
- 44 Koliaki, C., Liatis, S., Dalamaga, M. & Kokkinos, A. The Implication of Gut Hormones in the Regulation of Energy Homeostasis and Their Role in the Pathophysiology of Obesity. *Curr Obes Rep* **9**, 255-271 (2020). <https://doi.org:10.1007/s13679-020-00396-9>
- 45 Moran, A. W., Daly, K., Al-Rammahi, M. A. & Shirazi-Beechey, S. P. Nutrient sensing of gut luminal environment. *Proc Nutr Soc* **80**, 29-36 (2021). <https://doi.org:10.1017/S0029665120007120>
- 46 Liu, J., Yu, K. & Zhu, W. Amino acid sensing in the gut and its mediation in gut-brain signal transduction. *Anim Nutr* **2**, 69-73 (2016). <https://doi.org:10.1016/j.aninu.2016.03.007>
- 47 Laeger, T. *et al.* FGF21 is an endocrine signal of protein restriction. *J Clin Invest* **124**, 3913-3922 (2014). <https://doi.org:10.1172/JCI74915>
- 48 Lu, J. *et al.* Sestrin is a key regulator of stem cell function and lifespan in response to dietary amino acids. *Nat Aging* **1**, 60-72 (2021). <https://doi.org:10.1038/s43587-020-00001-7>
- 49 Richardson, N. E. *et al.* Lifelong restriction of dietary branched-chain amino acids has sex-specific benefits for frailty and lifespan in mice. *Nat Aging* **1**, 73-86 (2021). <https://doi.org:10.1038/s43587-020-00006-2>
- 50 Zhang, Y. *et al.* The starvation hormone, fibroblast growth factor-21, extends lifespan in mice. *Elife* **1**, e00065 (2012). <https://doi.org:10.7554/eLife.00065>
- 51 Park, T. J. *et al.* Somatosensory organization and behavior in naked mole-rats: II. Peripheral structures, innervation, and selective lack of neuropeptides associated with thermoregulation and pain. *J Comp Neurol* **465**, 104-120 (2003). <https://doi.org:10.1002/cne.10824>
- 52 Lian, T. *et al.* *Drosophila* Gut-A Nexus Between Dietary Restriction and Lifespan. *Int J Mol Sci* **19** (2018). <https://doi.org:10.3390/ijms19123810>

- 53 Piper, M. D., Partridge, L., Raubenheimer, D. & Simpson, S. J. Dietary restriction and aging: a unifying perspective. *Cell Metab* **14**, 154-160 (2011). <https://doi.org:10.1016/j.cmet.2011.06.013>
- 54 Solon-Biet, S. M. *et al.* The ratio of macronutrients, not caloric intake, dictates cardiometabolic health, aging, and longevity in ad libitum-fed mice. *Cell Metab* **19**, 418-430 (2014). <https://doi.org:10.1016/j.cmet.2014.02.009>
- 55 Lopez-Otin, C., Blasco, M. A., Partridge, L., Serrano, M. & Kroemer, G. The hallmarks of aging. *Cell* **153**, 1194-1217 (2013). <https://doi.org:10.1016/j.cell.2013.05.039>
- 56 Tennessen, J. M., Barry, W. E., Cox, J. & Thummel, C. S. Methods for studying metabolism in *Drosophila*. *Methods* **68**, 105-115 (2014). <https://doi.org:10.1016/j.ymeth.2014.02.034>
- 57 Wong, R., Piper, M. D. W., Wertheim, B. & Partridge, L. Quantification of Food Intake in *Drosophila*. *PLOS ONE* **4**, e6063 (2009). <https://doi.org:10.1371/journal.pone.0006063>
- 58 Arsic, A., Stajkovic, N., Spiegel, R. & Nikic-Spiegel, I. Effect of Vectashield-induced fluorescence quenching on conventional and super-resolution microscopy. *Sci Rep* **10**, 6441 (2020). <https://doi.org:10.1038/s41598-020-63418-5>
- 59 Marchetti, M., Zhang, C. & Edgar, B. A. An improved organ explant culture method reveals stem cell lineage dynamics in the adult *Drosophila* intestine. *Elife* **11** (2022). <https://doi.org:10.7554/eLife.76010>
- 60 Schindelin, J. *et al.* Fiji: an open-source platform for biological-image analysis. *Nature methods* **9**, 676-682 (2012). <https://doi.org:10.1038/nmeth.2019>
- 61 Tennessen, J. M., Barry, W. E., Cox, J. & Thummel, C. S. Methods for studying metabolism in *Drosophila*. *Methods* **68**, 105-115 (2014). <https://doi.org:10.1016/j.ymeth.2014.02.034>

Supplementary Files

This is a list of supplementary files associated with this preprint. Click to download.

- [SupplementaryTableS1.docx](#)
- [SupplementaryTableS2.docx](#)
- [Extendeddata.pdf](#)